MIT Open Access Articles

Organic Matter Loading Modifies the Microbial Community Responsible for Nitrogen Loss in Estuarine Sediments

1   **Organic matter loading modifies the microbial community responsible for nitrogen loss in**

2   **estuarine sediments**

3

4

5   Andrew R. Babbin[a,b]#, Amal Jayakumar[a], Bess B. Ward[a]

6

7   Department of Geosciences, Princeton University, Princeton, NJ, USA[a];

8   Department of Civil & Environmental Engineering, MIT, Cambridge, MA, USA[b]

9

10   #Correspondence to Andrew R. Babbin, babbin@mit.edu.

11

13

1 **Abstract**

2 Coastal marine sediments, as locations of substantial fixed nitrogen loss, are very important to

3 the nitrogen budget and to the primary productivity of the oceans. Coastal sediment systems are

4 also highly dynamic and subject to periodic natural and anthropogenic organic substrate

5 additions. The response to organic matter by the microbial community involved in nitrogen loss

6 processes was evaluated using mesocosms of Chesapeake Bay sediments. Over the course of a

7 50-day incubation, rates of anammox and denitrification were measured weekly using ^{15}N tracer

8 incubations, and samples were collected for genetic analysis. Rates of both nitrogen loss

9 processes and gene abundances associated with them corresponded loosely, probably because

10 heterogeneities in sediments obscured a clear relationship. The rates of denitrification were

11 stimulated more, and the fraction of nitrogen loss attributed to anammox slightly reduced, by the

12 higher organic matter addition. Furthermore, the large organic matter pulse drove a significant

13 and rapid shift in the denitrifier community composition as determined using a *nirS* microarray,

14 indicating the diversity of these organisms plays an essential role in responding to anthropogenic

15 inputs. We also suggest that the proportion of nitrogen loss due to anammox in these coastal

16 estuarine sediments may be underestimated due to temporal dynamics as well as from

17 methodological artifacts related to conventional sediment slurry incubation approaches.

18

19 **Introduction**

20   Coastal and estuarine sediments are environments of intense loss of fixed nitrogen

21 through the microbial processes of denitrification and anaerobic ammonium oxidation

22 (anammox). Globally, these areas can account for up to three-quarters of the fixed nitrogen lost

23 from the marine system [1−3]. Direct measurement of the fixed nitrogen loss rates is difficult,

24 however, because of significant spatial and temporal heterogeneities characteristic of sediments.

25 For instance, oxic or anoxic microsites [4] and an uneven distribution of organic matter create

26 pockets of reduced or enhanced nitrogen cycling, while episodic bloom-derived settling events of

27 organic matter onto sediment beds can lead to spikes in nitrogen loss rates [5]. How the

28 microbial community of denitrifiers and anammox bacteria responds to this sudden input of

29 organic matter in terms of biological rates and community composition is a crucial question in

30 better understanding these dynamic and climatically relevant sediment systems.

31　　　Increased fixed nitrogen levels are typically associated with coastal estuarine systems

32 such as Chesapeake Bay, where higher concentrations of ammonium and urea are measured

33 following spring storm events [6–8]. During these periods, fertilizer applied to croplands runs off

34 into the tidal estuary, and causes phytoplankton blooms which in turn deposit on the sediment

35 bed. Aquaculture in cages or pens also contributes high organic loading in some systems.

36 Additionally, discharge of sewage, either by inadequate treatment facilities or through combined

37 sewage overflow, is another avenue by which nitrogen is directly injected into the coastal

38 environment. These transient pulses consist of high concentrations of ammonium, nitrate, and

39 labile particulate organic matter [6, 9, 10]. The link between these events and the microbial

40 community that consumes this nitrogen is therefore key in understanding the amplitude of the

41 response of the coastal system to anthropogenically-derived nitrogen.

42　　　Denitrification, anammox and dissimilatory nitrate reduction to ammonium (DNRA) are

43 all involved in nitrogen removal from sediments. The major consumption of fixed nitrogen in

44 natural estuarine sediments is denitrification [11, 12], the heterotrophic stepwise reduction of

45 nitrate or nitrite to nitrous oxide and dinitrogen gas via a series of reductase enzymes. Of the

46 multiple enzymes in this sequence, nitrite reductase, which converts nitrite to nitric oxide is the

47 most critical in that it is the one that leads rapidly to loss of fixed nitrogen from the environment.

48 This enzyme is encoded by *nirS*, a diverse gene commonly found in denitrifiers [13], or by *nirK,*

49 which encodes a metabolically equivalent but structurally distinct enzyme. In Chesapeake Bay

50 and other estuarine systems, however, *nirK* has been difficult to detect and is consistently found

51 at much lower copy numbers [14–18], making *nirS* the more useful functional biomarker gene

52 for denitrification in Chesapeake Bay. In estuarine environments, much of the organic matter,

53 which is required for denitrification, is highly refractory [19], with a C/N ratio > 9 and not

54 readily solubilized. The anthropogenic addition of labile easily-solubilized organic molecules

55 may therefore enhance denitrification rates when nitrate is present [20–22].

56   Anammox too removes fixed nitrogen from certain sediment environments [23, 24]. Still,

57 anammox was minimal in trout aquaculture settlement ponds [25] and a rare but significant

58 contribution in shrimp aquaculture ponds [26]. It was also reported to be a minor nitrogen loss

59 process in three U.S. east coast estuaries, Chesapeake Bay [11], Cape Fear [27], and Providence

60 River [28]. These low rates imply a limited significance for DNRA-coupled nitrogen loss

61 whereby anammox consumes ammonium provided in situ by DNRA. Anammox, an autotrophic

62 process by which ammonium is oxidized anaerobically using nitrite as an electron acceptor, is

63 constrained by similar dissolved oxygen and DIN controls as denitrification despite

64 fundamentally different metabolisms. Anammox requires both reduced (ammonium) and

65 oxidized (nitrite) forms of nitrogen, which do not usually co-occur in space or time due to (1) the

66 ability of nitrification to aerobically oxidize ammonium even with limited amounts of oxygen

67 [29–31], and (2) the reduction of nitrite via denitrification using high C/N organic matter

68 substrate reserves in sediments. Given a large enough pulse of reduced inorganic (i.e.

69 ammonium) or organic nitrogen, however, anammox may be able to utilize these conditions to

70 couple with nitrification and/or heterotrophic nitrate reduction to remove ammonium rapidly

71 [32]. In this sense, both anammox and denitrification can be controlled by the same organic and

72 inorganic nitrogen substrates, and can be stimulated by their injection into the estuarine system.

73   Ammonium is the critical link in constraining rates of sedimentary anammox and

74 denitrification because it does not accumulate sufficiently in the anoxic depth layers of active

75 nitrogen loss [33, 34]. Therefore, barring physical transport, mass balance on ammonium implies

76 that anammox consuming NH_4^+ and denitrification producing it should occur in specific ratios

77 set by the stoichiometry of organic matter fueling nitrate reduction and denitrification.

78 Analogous stoichiometry-dependent coupling has been shown in the anoxic water column [35],

79 and is also likely important in anoxic sediments [5, 36]. For instance, if the material reaching the

80 sediments is of average marine phytoplankton composition (C/N = 6.6), anammox should

81 account for 29% of the fixed nitrogen loss [37]. This anammox proportion, however, should vary

82 with organic nitrogen content relative to carbon fueling the microbial community: more nitrogen

83 corresponds to higher amounts of anammox relative to denitrification. Additional allochthonous

84 NH_4^+ supplied through runoff or from remineralization in deeper sediments via processes such as

85 sulfate reduction could further amplify the anammox contribution, as observed in deep sea

86 sediments off the Washington margin [24].

87   We used an incubation approach in order to reduce natural variability and to test the

88 effect of organic matter on the rates of fixed nitrogen loss in the absence of other variables.

89 Using replicate sediment mesocosms, we controlled the supply of organic and inorganic

90 nutrients. Although the mesocosms do not simulate the actual system response to a bloom setting

91 event or pulses of inorganic nutrients, they allow us to investigate the mechanisms and directions

92 of change that might occur in the natural estuarine system. We measured the time dependence of

93   nitrogen loss rates and gene abundances for anammox (*16S rRNA*) and denitrification (*nirS*

94   functional gene) following an injection of ammonium, nitrate, and two levels of organic matter.

95   We further used the diversity of the *nirS* gene as determined from a microarray analysis to

96   quantify the denitrifier community response to the organic substrate pulse at two different levels.

97

98   **Materials and Methods**

99   *Mesocosm design*

100   The mesocosm experiments, as previously described by Babbin and Ward [5], were

101   seeded with sediments and site water from the lower Choptank River in the Chesapeake Bay

102   estuary (station CT2, 38°37.191′ N 76°08.061′ W, station depth = 7.9, salinity = 14) collected in

103   November 2009. Briefly, homogenized sediments were divided into four replicate containers

104   (cross-section of 40 cm × 25 cm) forming a layer ~2.5 cm in thickness, and overlain with ~18.5

105   cm of site water. The sediments were pre-incubated for six months to remove any preexisting

106   labile substrates before nitrate and ammonium in the overlying water were restored to near-

107   original concentrations, and organic matter in the form of commercially available fish food (C/N

108   = 4.2; Tetrafin, Blacksburg, VA) was applied to the surface of the sediments. Two of the

109   mesocosms (L1 and L2) received 0.4 mg cm^{-2} organic matter, and two (H1 and H2) received a

110   10-fold higher addition of 4.0 mg cm^{-2}. The level of organic matter addition was chosen to

111   provide a large signal in the biogeochemical and microbial community response, and similar to

112   previous mesocosm studies, e.g., [38, 39]. The organic matter amendment was raked across the

113   surface of the sediments in order to seed the approximate depth zone (upper few millimeters) of

114   the active nitrogen cycle and to mimic a natural deposition event such as might occur after a

115   phytoplankton bloom.

116   The mesocosms were incubated for seven weeks in the dark at room temperature

117   following the organic matter additions. The overlying water was aerated and mixed by gently

118   bubbling with air, which also prevented the build up of sulfide (sulfide was never sensed over the

119   course of the incubation). Overlying water was sampled daily for dissolved inorganic nitrogen

120   (DIN), measured using standard techniques [5]. Periodically, the mesocosm sediments were also

121   sampled for instantaneous rate experiments and DNA by coring an entire 2.5 cm sediment plug,

122   homogenizing, and aliquoting into incubation vials for isotope labeling experiments (rate

123   measurements) or Nalgene cryovials and frozen at −80 °C (DNA) [17].

124

125   *Rate experiments*

126   Three full-depth sediment cores (90% porosity) were collected from each mesocosm

127   using a syringe into a 20 mL vial. The vials were then homogenized in an Argon-flushed glove

128   bag, and 1.5 mL subsamples were aliquoted into 5.9 mL Exetainers (Labco, UK), similar to

129   previous studies [11, 40]. Concentrated stocks of [^{15}N]-labeled NH_4^+ or NO_2^- were added (final

130   amendment of 4 nmol N), and the vials capped. The Exetainers were vortexed briefly to

131   distribute the tracer, and flushed on a gas purging manifold at 5 psi of Argon for 5 minutes.

132   Triplicate vials were killed with 100 µL 50% (w/v) $ZnCl_2$ solution at time points of 0 and 30

133   min. Production of labeled [^{15}N]-N_2 gas from the ammonium and nitrite treatments were

134   measured on a Delta V Plus IRMS (ThermoScientific) at the UC Davis Stable Isotope Facility.

135   The incubation time of 30 minutes was determined as appropriate for linear production of N_2

136   from previous experiments in Chesapeake Bay [11].

137   After analysis for gases, 2 mL of 2 mol L^{-1} KCl solution was added to the sediment

138   slurry, and vials shaken on a reciprocal shaker for 12 hours at 100 rpm. The slurries were then

139   centrifuged (2000×g, 5 min) and supernatant collected and frozen until analysis. NH_4^+ was

140   measured using fluorometry after conversion with orthophthaldialdehyde [41] and NO_2^- with

141   standard spectrophotometric techniques [42]. These concentrations, generally below detection

142   (data not shown), were used to determine fraction of substrate labeled to calculate the nitrogen

143   loss rates (e.g., 11, 31).

144

145   *DNA extraction and quantitative PCR amplification*

146   DNA from mesocosms L1 and H1 was extracted in duplicate from 0.5 g (wet weight)

147   sediment aliquots (temperature = 25 °C, pH = 8, salinity = 14) using the MoBio PowerSoil®

148   DNA Isolation Kit (MoBio Laboratories, Carlsbad, CA) following manufacturer's protocols.

149   Duplicate extracts were then pooled for qPCR analysis. Methods of qPCR using SYBR Green

150   for *nirS* and anammox *16S rRNA* genes, and the standardization and verification of specificity

151   for qPCR assays were performed as described previously [43]. The efficiency of the qPCR

152   reactions was calculated using the slopes of the standard curves, and was 77% for anammox *16S*

153   *rRNA* assay and 107% for *nirS* assay. The amplified products were visualized after

154   electrophoresis in 1% agarose gels stained with ethidium bromide. Standards for PCR

155   quantification of each fragment were prepared by amplifying a constructed plasmid containing

156   the respective gene fragment, followed by quantification and serial dilution.

157   Assays of each gene for all four samples were carried out within a single assay plate [44].

158   Each assay included triplicates of the no template controls, no primer control, five (*nirS*) or

159   seven (anammox *16S rRNA*) standards, and triplicates of known quantity of the environmental

160   DNA samples (20 – 25 ng). DNA was quantified using PicoGreen fluorescence (Molecular

161   Probes, Eugene, OR) calibrated with several dilutions of phage lambda standards and qPCR was

162   performed using a Stratagene MX3000P (Agilent Technologies, La Jolla, CA). Automatic

163   analysis settings were used to determine the threshold cycle (Ct) values.

164

165   *nirS microarray analysis*

166   The array (BC014) was developed with the archetype array approach described and

167   conducted previously [45, 46] with 90-mer oligonucleotide probes. Each probe consisted of a

168   *nirS*-specific 70-mer region and a 20-mer control region (5′-GTACTACTAGCCTAGGCTAG-

169   3′) bound to a glass slide. The design and spotting of the probes has been described previously

170   [47, 48]. BC014 contains 164 *nirS* archetype probes representing ~2000 sequences from a range

171   of environments, including both sediments and oxygen deficient zone water columns, that were

172   publicly available in November 2009 when the array was designed (the probe accession numbers

173   and sequences are described elsewhere) [46]. The probes differ from each other by ~15%

174   sequence identity, the level at which cross hybridization is insignificant [47].

175   Array analysis was performed as described previously [46, 49] with some modifications.

176   Triplicate qPCR *nirS* gene fragment amplicons were pooled, gel purified, and labeled with

177   amino-allyl-dUTP (Life Technologies) during linear amplification using random octamers and a

178   Klenow polymerase (Invitrogen). The reaction contained 3.9 mmol L^{-1} d(AGC)TP, 0.4 mmol L^{-1}

179   dTTP, and 4.8 mmol L^{-1} dUaa, and was carried out at 37 °C for 3 hours. The Klenow product

180   was purified by precipitation and conjugated with Cy3 dye. The Cy3-labelled target (200 ng) was

181   combined with hybridization buffer (Agilent) and 0.25 pmol of a Cy5-labelled complementary

182   20-mer standard oligonucleotide then incubated at 95 °C for 5 min before being cooled to room

183   temperature. Targets were hybridized to duplicate or triplicate arrays by overnight incubation at

184   64 °C and washed. The arrays were scanned with a laser scanner (Molecular Devices 4300) and

185   analyzed with Gene Pix Pro 6.0 software (Molecular Devices). Quantification of hybridization

186   signals was performed as described previously [46] including the following quality controls for

187   signal reproducibility. For each channel, i.e. 532 nm (Cy3) and 635 nm (Cy5), the average

188   background fluorescence was recalculated after excluding background fluorescence values

189   greater than the upper whisker of all of the background fluorescences. This limit was defined as

190   the 75th percentile plus 1.5 times the interquartile range. Such a filtering process was applied

191   within each block on a microarray to account for variability in background fluorescence between

192   blocks within an array.

193   Then a normalized fluorescence ratio (FRn) for each archetype was calculated by

194   dividing the fluorescence signal of the archetype by the highest fluorescence signal within the

195   same array, and the FRn of each archetype from the replicate arrays was averaged. The relative

196   fluorescence ratio (RFR) of each archetype was calculated as the contribution of FRn of the

197   archetype to the cumulative sum of FRn of all *nir*S archetypes on the array and averaged for

198   replicate arrays from each sample. The original array data are available at Gene Expression

199   Omnibus (http://www.ncbi.nlm.nih.gov/projects/geo/) at the National Center for Biotechnology

200   Information under GEO Accession Number GSE65430.

201   The array data were analyzed using the 'vegan' package in R (http://www.R-project.org)

202   [50]. Archetypes contributing less than 1% of the total signal in all samples were removed from

203   further analysis. RFR values ≥ 1% were arcsine–square root transformed to normalize the

204   proportional data. Environmental data were square root transformed and then standardized

205   around zero (decostand in vegan). The transformed data were used in all diversity and correlation

206   analyses according to Borcard et al. [50].

207

208 **Results**

209 *Mesocosm DIN concentrations over time*

210   The progression of the different DIN species – NH_4^+, NO_2^-, and NO_3^- – measured in the

211 water overlying the sediments in the mesocosms has been published in detail previously [5]. To

212 provide context for the experimental data presented here, however, the DIN results are

213 summarized. The two levels of organic matter addition stimulated different magnitudes and

214 timings of mineralization, DIN accumulation, associated nitrification and nitrogen loss (Fig. 1).

215 The overall progression of the two treatments was similar, however, proceeding from a state

216 dominated by ammonium to one more oxidized and comprised mostly of nitrate. The total DIN

217 concentration decreased concurrently with this shift from ammonium- to nitrate-dominance,

218 providing evidence of co-occurring nitrogen loss during the nitrification phase.

219

220 *Nitrogen loss rates*

221   The rates of anammox and denitrification measured directly in slurries from mesocosm

222 sediments varied with time (Fig. 2). In the low organic matter mesocosms, the denitrification rate

223 was generally higher than the anammox rate (up to ~10 nmol N g^{-1} d^{-1}) but did not fluctuate

224 reproducibly. The anammox rate, however, was consistently low (< 4 nmol N g^{-1} d^{-1}) except for a

225 peak rate of 5 and 8 nmol N g^{-1} d^{-1} in L1 and L2 respectively, toward the end of the incubations.

226 These two mesocosms showed similar trends in the rate time courses, but with a time offset, with

227 L2 lagging L1. This lag was also evident in the DIN concentration time series.

228   The mesocosms subjected to a high organic matter amendment (Fig. 2C, D) showed a

229 very different trend in the rate measurements. Here, the anammox rates generally were lower

230 than in L1 and showed no significant peak. Further, both H1 and H2 showed dual maxima (up to

231 20 nmol g^{-1} d^{-1}) in denitrification: one at the beginning of the experiments, just following the

232 organic matter addition, and one toward the end of the incubations. In the previous model

233 analysis, we found that the rates of all biological processes increased in concert with each other,

234 making the percentage of nitrogen loss attributed to anammox consistent regardless of treatment

235 (44.3 ± 0.3% anammox) [5]. From the direct measurements presented here, however, we found

236 the anammox percentages to be lower than the modeled value: 32 ± 8% (SE) for the L

237 mesocosms and 27 ± 8% for the H mesocosms.

238

239 *Denitrifier nirS and anammox 16S rRNA gene abundances*

240　　　　Because the replication between duplicate mesocosms was very consistent for both

241 treatments, genetic analysis was conducted on sediment DNA extracts from only one mesocosm

242 from each organic treatment, L1 and H1 (Fig. 3). Tank L1 did not show a trend in abundance of

243 the denitrifier *nirS* functional gene, with an average of $6.6 ± 0.4 × 10^7$ (SD) gene copies g^{-1} wet

244 sediment. For anammox *16S rRNA*, however, while the total abundance was an order of

245 magnitude lower than *nirS*, there was a significant ~4-fold increase from 2.5 to $10 × 10^6$ copies

246 g^{-1} wet sediment between days 10 and 30. This increase in the single copy gene implies a

247 doubling time of 10 days for the anammox community over this time period, similar to previous

248 estimates [51, 52]. The number of gene copies then decreased back toward initial levels. Tank

249 H1 showed the opposite pattern compared with L1: there was no significant trend in the

250 anammox *16S rRNA* gene abundances, averaging $3.5 ± 1.4 × 10^6$ copies g^{-1} wet sediment over

251 the time course of the incubation. The denitrifier *nirS* abundance, however, started relatively

252 high (and at the same level as that in L1), approximately $6 × 10^7$ copies g^{-1} wet sediment before

253 decreasing until day 16 and then peaking at over 10^8 copies g^{-1} wet sediment on day 38. These

254   peak abundances in anammox *16S rRNA* in L1 and *nirS* in H1 are significantly greater than the

255   abundances in the remainder of their respective time courses ($p < 10^{-7}$).

256

257   *Denitrifier community diversity*

258   Based on the denitrification rate and *nirS* gene abundance peaks in H1 at day 38, we

259   investigated whether there was a shift in the community associated with these increases. Such a

260   shift could take the shape of a few dominants or a single winner, or a less obvious change in the

261   overall community composition of the major (> 1% of total) groups. Only 39 of the 164

262   archetype probes were detected as a major component of at least one sample, and the major

263   groups comprised 66.4%, 54.7%, 46.3%, and 54.0% of the total microarray fluorescence for L1-

264   3, L1-38, H1-3, and H1-38 samples respectively (Fig. 4). These data also show that the major

265   *nirS* community in both treatments at both the beginning (day 3) and near the end (day 38) were

266   not dominated by a single winner. Both Shannon diversity ($H = 3.01 \pm 0.02$) and evenness ($E =$

267   0.95 ± 0.01) indices were relatively high and showed little variation across organic matter

268   treatments and time points and indicated a diverse community. However, the community

269   comprising the major groups (those that accounted for > 1% of the total signal) was different

270   among the samples. The Bray-Curtis dissimilarity index (not shown) indicated that the two days

271   sampled from L1 were more similar to each other than to either day in H1, although all four

272   communities were not statistically different due to the abundance of the major groups. H1-3 was

273   most similar to L1-3; and, the most dissimilar samples were L1-38 and H1-38. These results

274   indicate a divergence in community over the 38 days of the incubations caused by the application

275   of labile organic matter.

276   The composition of the community shift is interesting, and can be delineated based on

277   occurrence in subsets of tanks and times. There were 12 archetypes that represented a major part

278   of the total signal in both tanks at both the beginning and end. Eight of these archetypes represent

279   sequences derived from the Choptank River (Nir71, 5, 134, 115, 82, 33, 150, 112), two from

280   elsewhere in Chesapeake Bay (Nir28, 164), one from the coastal Arabian Sea water column

281   (Nir111), and one (Nir1; *Pseudomonas aeruginosa*) which is found in many environments

282   including Chesapeake Bay sediments and the Arabian Sea oxygen deficient waters [53]. These

283   twelve archetypes comprise a large fraction of the major groups (L1-3: 78%, L1-38: 70%, H1-3:

284   73%, H1-38: 65%) but, interestingly, account for 8% less of the total after 38 days of incubation

285   with the organic matter amendments.

286   Upon incubation with a high amount of organic carbon, however, the relative

287   hybridization signal of some groups decreased, and others increased. Archetypes Nir148 and

288   Nir80, which existed in approximately equal proportions at both time points in L1 and in H1-3,

289   and five of the major archetypes in H1-3 were not major components of the community in H1-

290   38. Moreover, eight archetypes, which comprised 18% of that sample's signal, were found only

291   in sample H1-38 (Fig. 4). The most important of these, archetype 123, made up more than 8% of

292   H1-38's signal. This sequence was derived from site CB1 in Chesapeake Bay when/where the

293   measured fixed nitrogen loss rates were highest among all sites analyzed [16]. While the

294   sequence is not closely related to any known organism, it groups with sequences from highly

295   productive systems: Baltic Sea, oxygen deficient zones, and during cyanobacteria blooms [16].

296   In a principal component analysis of the microarray data, the first two principal

297   components explain 50% and 34% of the variance, respectively (Fig. 5). Samples L1-3 and L1-

298   38 are clustered whereas H1-3 and H1-38 are approximately equidistant from the L1 samples.

299   The differences between the average of the two L1 samples ($\overline{\text{L1}}$) and H1-3 are due to both PC1

300   and PC2, but $\overline{\text{L1}}$ and H1-38 differ only along PC1. The geometric distance in PC1/PC2 space

301   between $\overline{\text{L1}}$ and H1-3 is less than that between $\overline{\text{L1}}$ and H1-38, confirming the greater similarity

302   between the initial communities in the low and high carbon mesocosms before the addition of

303   organic matter. It is worth noting that the distance between $\overline{\text{L1}}$ and H1-3 is in fact less than that

304   between H1-3 and H1-38 (3.9 compared to 4.7), which implies that the divergence of the

305   community during 6 months of pre-incubation was less than the shift observed in the period of

306   35 days following a large organic carbon amendment. A heatmap based on correlation analysis

307   of the combined RFR, qPCR and environmental data illustrates some relationships among

308   archetypes and other variables. The same archetype clusters are evident in the heatmap (Fig. 6)

309   and the PCA (Fig. 5). For example, *nirS* abundance was positively correlated with the archetype

310   cluster that includes Nir123, one of the archetypes that was significant only in H1 at D38, i.e., in

311   response to the high OM addition. Nir33, which was a significant archetype in the initial

312   samples, was correlated with high DIN concentrations. Nir21 did not cluster with other

313   archetypes but was the archetype with the highest correlation to denitrification rate.

314

315   **Discussion**

316   Organic matter, as might be derived from a phytoplankton bloom settling event or from

317   seasonal fish farming, induced changes in the nitrogen biogeochemistry observed in the

318   mesocosms. The high OM treatment showed elevated rates of denitrification, as would be

319   expected given the mainly heterotrophic nature of this process and its dependence on organic

320   carbon. Interestingly, however, the response appears bimodal, with the initial peak corresponding

321   to an immediate community response to the labile OM addition, and a second, month-later peak

14

322 upon the exhaustion of nitrite and the maximum nitrate concentration in the overlying water.

323 This temporal course of denitrification rates would indicate that the sediment biogeochemistry is

324 such that the denitrifiers will rapidly increase their rates when presented high amounts of labile

325 OM, but a byproduct, either NH_4^+, NO_2^-, or some other unmeasured biomarker, is produced to

326 hinder complete consumption of this OM. When this inhibition is removed, however, the

327 denitrifiers are able to increase their rates again and consume both OM and DIN. In the natural

328 environment, where the overlying water is flushed and replenished, such inhibition may not

329 occur, and the denitrifiers able to consume the organic matter addition much more rapidly.

330   This inhibition may also encompass competition with DNRA at high levels of dissolved

331 organic matter. As we added particulate organic matter to the pre-incubated mesocosms, there

332 should be a delay in solubilizing this organic amendment and allowing it to build up to levels

333 that thermodynamically favor nitrate reduction to ammonium rather than to N_2 [40, 54, 55].

334 However, dissolved organic matter levels were not monitored throughout the experiments, and

335 the controls on the partitioning between denitrification and DNRA are more complicated than

336 only organic carbon dependence [56, 57]. Our study does nonetheless imply complex dynamics

337 in the denitrifier population and metabolic rates, and necessitates further investigation into the

338 competition with other microbial communities.

339   The mesocosm experimental approach allows for the evaluation of how the microbiology

340 responds to an organic matter pulse in the absence of external forcing (e.g., flowing water in the

341 natural system). However, as is often true for sediments, even the mesocosms are subject to

342 heterogeneities and measurement artifacts that obscure the relationships among rates, DIN

343 concentrations, and DNA gene abundances. The peaks in directly measured rates of anammox

344 and denitrification do not consistently correspond either to peaks in the DIN concentrations or to

345 the modeled rates derived from them [5]. There are a number of possible explanations for this

346 discrepancy. First, the discrete rate measurements made once per week may miss actual peaks in

347 the rates. For instance, in the low organic matter mesocosms, small rate maxima that were

348 observed within the first 10 days might have corresponded more precisely to the modeled

349 maximum rate of ammonium consumption at days 8–9 had rate experiments been conducted on

350 those days.

351   Contributing to this lack of overall correlation is the fact that these sediment systems are

352 highly heterogeneous. The labile organic matter amendment was raked over the entire sediment

353 bed, but on the microscale where microbes operate [58], heterogeneities abound. As the systems

354 are driven by the organic material, its distribution is certainly crucial in controlling the small

355 scale locations of biological rates within a sediment matrix. The DIN measurements sampled the

356 homogenous water column overlying the entirety of the sediment bed and integrated the

357 sediment heterogeneity. This led to high reproducibility between duplicate mesocosms in

358 integrated rates modeled from the DIN patterns [5], but rates directly measured in sediment

359 incubations are subject to small scale heterogeneity and therefore less reproducible.

360   The directly measured rates presented here are lower than some literature reports, e.g.,

361 [59–61], but we note that our rates are not directly comparable. Our rates are averaged over the

362 entire 2.5 cm-thick sediment plug whereas the zone of denitrification is likely on the order of

363 one-tenth of that thickness [62]. Accounting for this factor of ten would make the rates reported

364 here on the same order as previous reports in other locations using other methods. Further, the

365 direct rate measurements are consistent with the magnitude of the observed nitrate drawdown.

366 For instance, nitrate was drawn down ~50 μmol L^{-1} in 10 d toward the end of the incubations

367 (Fig. 1), and given that the mesocosms comprised 2 kg of sediment and 20 L of water, this

368 equates to 50 nmol g^{-1} d^{-1}, again of the same magnitude as the peak rate measurements.

369   The slurry method used here also meant that the entire sediment column was cored and

370 homogenized in order to minimize artifacts from preferentially selecting only specific depth

371 layers [17]. This homogenization and redistribution of active nitrogen cycle bacteria and organic

372 matter from the interface into the whole core may have altered the proportions of N_2 generation

373 attributed to anammox and denitrification. While the organic matter amendment had a C/N of

374 4.2, there was a large background C/N of ~9 which is typical of recalcitrant organic matter in

375 estuarine systems [5, 19]. The newly applied organic material was mostly restricted to the active

376 nitrogen loss zone at the sediment water interface which fueled an anammox percentage of ~45%

377 when calculated from the overlying water (see Babbin and Ward [5]). When mixed and

378 redistributed with deeper, more N-depleted organic matter, however, the resulting proportion of

379 anammox was lower, and the average anammox contributions were $32 \pm 8\%$ (SE) and $27 \pm 8\%$

380 for the L and H mesocosms, respectively. This is in agreement with previous work [63] showing

381 that slurries tend to favor denitrification when compared with intact sediment cores, especially in

382 highly active sediments.

383   The measured denitrifier *nirS* and anammox *16S rRNA* gene abundances did not

384 consistently correspond with the instantaneous rates of fixed nitrogen loss. The lack of such a

385 correlation between *nirS* gene abundance with denitrification rates themselves has been seen in

386 other mesocosm experiments seeded with sediments from Eel Pond, Falmouth, MA [17]. There

387 are a number of factors besides presence of particular genes in the DNA that control biological

388 transformation rates and can obscure the relationship between biological rates and the organisms

389 responsible. Particularly, expression of the gene in RNA and substrate availability are important

17

390   in controlling the actual rates of denitrification. Moreover, homogenization over the whole

391   sediment column can obscure the signal by reducing overall rates and concentrations. Two of the

392   observed abundance maxima, where the signal was strongest, in anammox *16S* genes in L1 at

393   day 27 and *nirS* genes in H1 at day 38 nonetheless did correspond with maxima in directly

394   measured instantaneous rates. The same homogenized sediment slurry that was analyzed for the

395   rates was frozen for DNA extraction, so perhaps during these periods of especially high rates, the

396   signals in gene abundance reflect actual changes in abundance of the relevant microbes. The

397   inhomogeneity of individual sediment cores also likely contributes to lack of direct

398   correspondence between instantaneous rates and gene abundances. It is also very likely that the

399   primers we used did not detect all the members of the two functional groups. It is possible that

400   *nirK* denitrifiers contributed to the rates, but we did not investigate their abundance. The *nirS*

401   gene is very diverse and thus it is likely that some related genes escaped our detection.

402   Regarding anammox gene abundances, Van Kessel et al. [64] found that the dominant anammox

403   phylotype in biofilters in a freshwater aquaculture system was not closely related to known

404   anammox strains and thus would not have been detected with the standard 16S rRNA probes. It

405   is thus possible that anammox abundance detected here by 16S rRNA, was overestimated.

406   The community composition of the major denitrifiers determined from the *nirS*

407   microarray could be interpreted based on presence or absence of a few groups of archetypes. The

408   most abundant taxa were found in all four samples regardless of treatment or day of sampling

409   during the incubation. These 12 important groups derived almost exclusively from Choptank

410   River and Chesapeake Bay sequences and represented up to 52% of the total hybridization

411   signal. Their ubiquity underlines the reason for their importance: these groups exist at the mouth

412   of the Choptank River because they are favored by the environmental variability and conditions

18

413   (sediment type, organic matter composition and availability, inorganic nutrient concentrations,

414   and physicochemical factors like salinity) inherent to this location in the estuary. The dominance

415   of only a few archetypes is consistent with previous clone library work from Chesapeake Bay,

416   where only 8 of the 172 detected operational taxonomic units (defined as $\leq$ 5% dissimilarity)

417   were found to account for 42% of total *nirS* clones [16].

418   Because of the long pre-incubation before initiating the experiment by making the

419   nutrient additions, it is likely that the microbial assemblage at the first time point had diverged

420   from the natural assemblage in the bay at the time of sampling. Since all four mesocosms were

421   pre-incubated and both sets of treatment replicated very well in terms of net reaction rates [5],

422   the day 3 and day 38 samples are appropriate for investigating the effects of the different organic

423   amendments. In terms of overall community composition, there was no apparent change over the

424   35 days of mesocosm L1 in that almost all of the major groups that existed at day 3 still existed

425   at day 38. There was a shift in the community in terms of winners and losers from the

426   amendment of high organic matter, however. Near the end of the high organic matter

427   experiment, eight major archetypes that were unique to sample H1-38 and comprised 18% of the

428   total signal were detected. This appearance of new groups in H1 by day 38, and the

429   disappearance of 5 of 6 of the groups unique to H1 on day 3, indicate that minor groups initially

430   undetectable may become important should proper conditions arise. For instance, in this bloom-

431   like scenario, the initially rare archetype Nir123, which was found only in the high organic

432   matter treatment and represented more than 8% of H1-38's total signal, is likely a fast growing

433   group well suited to highly productive conditions. Such dominance of a few denitrifiers

434   responding to episodic environmental changes has also been shown in the Arabian Sea [43].

435   Archetype Nir123 exemplifies the importance rare taxa may have in transient settings. Without

436   these otherwise latent groups, sediment systems would not be able to respond as rapidly to pulse-

437   like events such as a settling bloom or anthropogenic discharge, and by extension, could not

438   buffer the coastal sea as readily from eutrophication.

439

440   *Conclusions*

441   The mesocosm experiments produced results similar to observations reported from the

442   natural Chesapeake Bay setting: greater importance of denitrification in terms of gene

443   abundances and biogeochemical rates compared with anammox, the presence of a small number

444   of highly important groups well-adapted to this system, and the growth of a specific winner

445   under certain eutrophic conditions. Bloom settling events, such as the one simulated here, induce

446   a dynamic cascade of nitrogen cycling processes and the microbial community responsible for

447   these transformations. The transience of a pulse of organic and inorganic nutrients induced a

448   high level of community evolution, stimulating as much divergence in one month as had

449   previously occurred in six months, despite little change in *nirS* gene abundance. Denitrifier

450   functional diversity apparently allows the coastal ecosystem community to adapt quickly and

451   ameliorate the effects of high nutrients and labile organic matter pulses.

452   This study also implies that the importance of anammox may in fact be underestimated

453   due to the use of the slurry incubation method, and even more importantly, due to the

454   significance of episodic organic loading in estuarine systems. The current paradigm in many

455   coastal systems is that denitrification accounts for upwards of 90% of fixed nitrogen loss [11,

456   28]. One explanation for this observation is that the high C/N composition of background

457   organic matter [19, 65, 66] favors denitrification without providing a significant ammonium

458   source for anammox. However, given the microbial response to an organic loading event

20

459   stimulated in the experiments presented here, periodic blooms should be disproportionately

460   important to both the overall nitrogen loss rates and the partitioning between anammox and

461   denitrification. As the organic matter deposited to the sediments would likely have a greater

462   nitrogen content than the refractory bulk, it is conceivable that the contribution of anammox

463   during times just following deposition and therefore to nitrogen loss as a whole in coastal

464   sediments is greater than previously thought.

465

466   **Acknowledgements**

475

References

477   1.   Brandes JA, Devol AH (2002) A global marine-fixed nitrogen isotopic budget:
478   Implications for Holocene nitrogen cycling. Global Biogeochem Cycles 16:1120. doi:
479   10.1029/2001GB001856

480   2.   Gruber N (2004) The dynamics of the marine nitrogen cycle and its influence on
481   atmospheric CO_2. In: Follows M, Oguz T (eds) Ocean Carbon Cycle Clim. Kluwer
482   Academic, Dordrecht, pp 97–148

483   3.   Codispoti LA (2007) An oceanic fixed nitrogen sink exceeding 400 Tg N a^{-1} vs the
484   concept of homeostasis in the fixed-nitrogen inventory. Biogeosciences 4:233–253.

485   4.   Brandes JA, Devol AH (1997) Isotopic fractionation of oxygen and nitrogen in coastal
486   marine sediments. Geochim Cosmochim Acta 61:1793–1801.

487   5.   Babbin AR, Ward BB (2013) Controls on Nitrogen Loss Processes in Chesapeake Bay
488   Sediments. Environ Sci Technol 47:4189–4196. doi: 10.1021/es304842r

489   6.   Glibert PM, Trice TM, Michael B, Lane L (2005) Urea in the tributaries of the
490   Chesapeake and Coastal Bays of Maryland. Water Air Soil Pollut 160:229–243.

491   7.   Lomas MW, Trice TM, Glibert PM, et al. (2002) Temporal and Spatial Dynamics of Urea
492   Uptake and Regeneration Rates and Concentrations in Chesapeake Bay. Estuaries 25:469–
493   482.

494   8.   Glibert PM, Harrison J, Heil C, Seitzinger S (2006) Escalating Worldwide use of Urea – A
495   Global Change Contributing to Coastal Eutrophication. Biogeochemistry 77:441–463. doi:
496   10.1007/s10533-005-3070-5

497   9.   Christensen PB, Rysgaard S, Sloth NP, et al. (2000) Sediment mineralization, nutrient
498   fluxes, denitrification and dissimilatory nitrate reduction to ammonium in an estuarine
499   fjord with sea cage trout farms. Aquat Microb Ecol 21:73–84.

500   10.   Lauer PR, Fernandez M, Fairweather PG, et al. (2009) Benthic fluxes of nitrogen and
501   phosphorus at southern bluefin tuna Thunnus maccoyii sea-cages. Mar Ecol Prog Ser
502   390:251–263.

503   11.   Rich JJ, Dale OR, Song B, Ward BB (2008) Anaerobic ammonium oxidation (Anammox)
504   in Chesapeake Bay sediments. Microb Ecol 55:311–320. doi: 10.1007/s00248-007-9277-3

505   12.   Koop-Jakobsen K, Giblin AE (2009) Anammox in Tidal Marsh Sediments: The Role of
506   Salinity, Nitrogen Loading, and Marsh Vegetation. Estuaries and Coasts 32:238–245. doi:
507   10.1007/s12237-008-9131-y

508   13.   Braker G, Zhou J, Wu L, et al. (2000) Nitrite Reductase Genes (nirK and nirS) as
509   Functional Markers To Investigate Diversity of Denitrifying Bacteria in Pacific Northwest
510   Marine Sediment Communities. Appl Environ Microbiol 66:2096–2104. doi:
511   10.1128/AEM.66.5.2096-2104.2000

512   14.   Abell GCJ, Revill AT, Smith C, et al. (2009) Archaeal ammonia oxidizers and nirS-type
513   denitrifiers dominate sediment nitrifying and denitrifying populations in a subtropical
514   macrotidal estuary. ISME J 4:286–300. doi: 10.1038/ismej.2009.105

515   15.   Mosier AC, Francis CA (2010) Denitrifier abundance and activity across the San
516   Francisco Bay estuary. Environ Microbiol Rep 2:667–676. doi: 10.1111/j.1758-
517   2229.2010.00156.x

518   16.   Francis CA, O'Mullan GD, Cornwell JC, Ward BB (2013) Transitions in nirS-type
519   denitrifier diversity, community composition, and biogeochemical activity along the
520   Chesapeake Bay estuary. Front Microbiol 4:237. doi: 10.3389/fmicb.2013.00237

521   17.   Bowen JL, Babbin AR, Kearns PJ, Ward BB (2014) Connecting the dots: Linking
522   nitrogen cycle gene expression to nitrogen fluxes in marine sediment mesocosms. Front
523   Microbiol 5:429. doi: 10.3389/fmicb.2014.00429

524   18.   Smith JM, Mosier AC, Francis CA (2014) Spatiotemporal Relationships Between the
525   Abundance, Distribution, and Potential Activities of Ammonia-Oxidizing and Denitrifying
526   Microorganisms in Intertidal Sediments. Microb Ecol N/A:N/A. doi: 10.1007/s00248-014-
527   0450-1

528   19.   Zimmerman AR, Canuel EA (2001) Bulk organic matter and lipid biomarker composition
529   of Chesapeake Bay surficial sediments as indicators of environmental processes. Estuar
530   Coast Shelf Sci 53:319–341. doi: 10.1006/ecss.2001.0815

531   20.   Middelburg JJ, Soetaert K, Herman PMJ, Heip CHR (1996) Denitrification in marine
532   sediments: A model study. Global Biogeochem Cycles 10:661–673.

533   21.   Cornwell JC, Kemp WM, Kana TM (1999) Denitrification in coastal ecosystems:
534   methods, environmental controls, and ecosystem level controls, a review. Aquat Ecol
535   33:41–54.

536   22.   Naqvi SWA, Jayakumar DA, Narvekar P V, et al. (2000) Increased marine production of
537   N2O due to intensifying anoxia on the Indian continental shelf. Nature 408:346–349.

538   23.   Dalsgaard T, Thamdrup B, Canfield DE (2005) Anaerobic ammonium oxidation
539   (anammox) in the marine environment. Res Microbiol 156:457–464. doi:
540   10.1016/j.resmic.2005.01.011

541 24. Engström P, Penton CR, Devol AH (2009) Anaerobic ammonium oxidation in deep-sea
542   sediments off the Washington margin. Limnol Oceanogr 54:1643–1652. doi:
543   10.4319/lo.2009.54.5.1643

544 25. Castine SA, Erler D V, Trott LA, et al. (2012) Denitrification and Anammox in Tropical
545   Aquaculture Settlement Ponds: An Isotope Tracer Approach for Evaluating N_2
546   Production. PLoS One 7:

547 26. Minjeaud L, Michotey VD, Garcia N, Bonin PC (2009) Seasonal variation in di-nitrogen
548   fluxes and associated processes (denitrification, anammox and nitrogen fixation) in
549   sediment subject to shellfish farming influences. Aquat Sci 71:425–435.

550 27. Lisa JA, Song B, Tobias CR, Duernberger KA (2014) Impacts of freshwater flushing on
551   anammox community structure and activities in the New River Estuary, USA. Aquat
552   Microb Ecol 72:17–31.

553 28. Brin LD, Giblin AE, Rich JJ (2014) Environmental controls of anammox and
554   denitrification in southern New England estuarine and shelf sediments. Limnol Oceanogr
555   59:851–860. doi: 10.4319/lo.2014.59.3.0851

556 29. Laanbroek HJ, Gerards S (1993) Competition for limiting amounts of oxygen between
557   Nitrosomonas europaea and Nitrobacter winogradskyi grown in mixed continuous
558   cultures. Arch Microbiol 159:453–459.

559 30. Kim J-G, Jung M-Y, Park S-J, et al. (2012) Cultivation of a highly enriched ammonia-
560   oxidizing archaeon of thaumarchaeotal group I.1b from an agricultural soil. Environ
561   Microbiol 14:1528–1543. doi: 10.1111/j.1462-2920.2012.02740.x

562 31. Martens-Habbena W, Berube PM, Urakawa H, et al. (2009) Ammonia oxidation kinetics
563   determine niche separation of nitrifying Archaea and Bacteria. Nature 461:976–979. doi:
564   10.1038/nature08465

565 32. Thamdrup B, Dalsgaard T (2002) Production of N2 through Anaerobic Ammonium
566   Oxidation Coupled to Nitrate Reduction in Marine Sediments. Appl Environ Microbiol
567   68:1312–1318. doi: 10.1128/AEM.68.3.1312-1318.2002

568 33. Bender M, Jahnke R, Weiss R, et al. (1989) Organic carbon oxidation and benthic
569   nitrogen and silica dynamics in San Clemente Basin, a continental borderland site.
570   Geochim Cosmochim Acta 53:685–697.

571 34. Kemp WM, Sampou P, Caffrey J, et al. (1990) Ammonium recycling versus
572   denitrification in Chesapeake Bay sediments. Limnol Oceanogr 35:1545–1563. doi:
573   10.4319/lo.1990.35.7.1545

574 35. Babbin AR, Keil RG, Devol AH, Ward BB (2014) Organic Matter Stoichiometry, Flux,
575   and Oxygen Control Nitrogen Loss in the Ocean. Science 344:406–408.

576   36.   Trimmer M, Engstrom P (2011) Distribution, activity, and ecology of anammox bacteria
577   in aquatic environments. In: Ward BB, Arp DJ, Klotz MG (eds) Nitrification. ASM Press,
578   Washington, D.C., pp 201–235

579   37.   Dalsgaard T, Canfield DE, Petersen J, et al. (2003) N_2 production by the anammox
580   reaction in the anoxic water column of Golfo Dulce, Costa Rica. Nature 422:606–608. doi:
581   10.1038/nature01526

582   38.   Caffrey JM, Miller LG (1995) A comparison of two nitrification inhibitors used to
583   measure nitrification rates in estuarine sediments. Fems Microbiol Ecol 17:213–220.

584   39.   Newell RIE, Cornwell JC, Owens MS (2002) Influence of simulated bivalve biodeposition
585   and microphytobenthos on sediment nitrogen dynamics: A laboratory study. Limnol
586   Oceanogr 47:1367–1379.

587   40.   Hardison AK, Algar CK, Giblin AE, Rich JJ (2015) Influence of organic carbon and
588   nitrate loading on partitioning between dissimilatory nitrate reduction to ammonium
589   (DNRA) and N_2 production. Geochim Cosmochim Acta 164:146–160. doi:
590   10.1016/j.gca.2015.04.049

591   41.   Holmes RM, Aminot A, Kérouel R, et al. (1999) A simple and precise method for
592   measuring ammonium in marine and freshwater ecosystems. Can J Fish Aquat Sci
593   56:1801–1808.

594   42.   Grasshoff K (1983) Determination of nitrite. In: Grasshoff K, Ehrhardt M, Kremling K
595   (eds) Methods seawater Anal., 2nd ed. Verlag Chemie, Weinheim, pp 143–150

596   43.   Jayakumar A, O'Mullan GD, Naqvi SWA, Ward BB (2009) Denitrifying bacterial
597   community composition changes associated with stages of denitrification in oxygen
598   minimum zones. Microb Ecol 58:350–362.

599   44.   Smith CJ, Nedwell DB, Dong LF, Osborn AM (2006) Evaluation of quantitative
600   polymerase chain reaction-based approaches for determining gene copy and gene
601   transcript numbers in environmental samples. Environ Microbiol 8:804–815. doi:
602   10.1111/j.1462-2920.2005.00963.x

603   45.   Ward BB, Bouskill NJ (2011) The utility of functional gene arrays for assessing
604   community composition, relative abundance, and distribution of ammonia-oxidizing
605   bacteria and archaea. Methods Enzymol 496:373–396. doi: 10.1016/b978-0-12-386489-
606   5.00015-4

607   46.   Jayakumar A, Peng X, Ward BB (2013) Community composition of bacteria involved in
608   fixed nitrogen loss in the water column of two major oxygen minimum zones in the ocean.
609   Aquat Microb Ecol 70:245–259. doi: 10.3354/ame01654

610   47.   Taroncher-Oldenburg G, Griner EM, Francis CA, Ward BB (2003) Oligonucleotide
611   Microarray for the Study of Functional Gene Diversity in the Nitrogen Cycle in the
612   Environment. Appl Environ Microbiol 69:1159–1171. doi: 10.1128/AEM.69.2.1159-
613   1171.2003

614   48.   Bulow SE, Francis CA, Jackson GA, Ward BB (2008) Sediment denitrifier community
615   composition and nirS gene expression investigated with functional gene microarrays.
616   Environ Microbiol 10:3057–3069. doi: 10.1111/j.1462-2920.2008.01765.x

617   49.   Peng X, Jayakumar A, Ward BB (2013) Community composition of ammonia-oxidizing
618   archaea from surface and anoxic depths of oceanic oxygen minimum zones. Front
619   Microbiol 4:177. doi: 10.3389/fmicb.2013.00177

620   50.   Borcard D, Gillet F, Legendre P (2011) Numerical Ecology with R. Springer, New York

621   51.   Strous M, Heijnen JJ, Kuenen JG, Jetten MSM (1998) The sequencing batch reactor as a
622   powerful tool for the study of slowly growing anaerobic ammonium-oxidizing
623   microorganisms. Appl Microbiol Biotechnol 50:589–596.

624   52.   Van der Star WRL, van de Graaf MJ, Kartal B, et al. (2008) Response of Anaerobic
625   Ammonium-Oxidizing Bacteria to Hydroxylamine. Appl Environ Microbiol 74:4417–
626   4426. doi: 10.1128/AEM.00042-08

627   53.   Jayakumar DA, Francis CA, Naqvi SWA, Ward BB (2004) Diversity of nitrite reductase
628   genes (nirS) in the denitrifying water column of the coastal Arabian Sea. Aquat Microb
629   Ecol 34:69–78.

630   54.   Porubsky WP, Weston NB, Joye SB (2009) Benthic metabolism and the fate of dissolved
631   inorganic nitrogen in intertidal sediments. Estuar Coast Shelf Sci 83:392–402. doi:
632   10.1016/j.ecss.2009.04.012

633   55.   Algar CK, Vallino JJ Predicting microbial nitrate reduction pathways in coastal sediments.
634   Aquat Microb Ecol 71:223–238.

635   56.   Kraft B, Tegetmeyer HE, Sharma R, et al. (2014) The environmental controls that govern
636   the end product of bacterial nitrate respiration. Science 345:676–9. doi:
637   10.1126/science.1254070

638   57.   Behrendt A, Tarre S, Beliavski M, et al. (2014) Effect of high electron donor supply on
639   dissimilatory nitrate reduction pathways in a bioreactor for nitrate removal. Bioresour
640   Technol 171:291–297. doi: 10.1016/j.biortech.2014.08.073

641   58.   Stocker R (2012) Marine Microbes See a Sea of Gradients. Science 338:628–633. doi:
642   10.1126/science.1208929

643 59. Joye SB, Smith S V., Hollibaugh JT, Paerl HW (1996) Estimating denitrification rates in
644   estuarine sediments: A comparison of stoichiometric and acetylene based methods.
645   Biogeochemistry 33:197–215. doi: 10.1007/BF02181072

646 60. Teixeira C, Magalhäes C, SB J, A BA (2012) Potential rates and environmental controls
647   of anaerobic ammonium oxidation in estuarine sediments. Aquat Microb Ecol 66:23–32.

648 61. Song GD, Liu SM, Marchant H, et al. (2013) Anammox, denitrification and dissimilatory
649   nitrate reduction to ammonium in the East China Sea sediment. Biogeosciences 10:6851–
650   6864. doi: 10.5194/bg-10-6851-2013

651 62. Risgaard-Petersen N, Nicolaisen MH, Revsbech NP, Lomstein BA (2004) Competition
652   between ammonia-oxidizing bacteria and benthic microalgae. Appl Environ Microbiol
653   70:5528–37. doi: 10.1128/AEM.70.9.5528-5537.2004

654 63. Trimmer M, Risgaard-Petersen N, Nicholls JC, Engström P (2006) Direct measurement of
655   anaerobic ammonium oxidation (anammox) and denitrification in intact sediment cores.
656   Mar Ecol Prog Ser 326:37–47.

657 64. Van Kessel MAHJ, Harhangi HR, van de Pas-Schoonen K, et al. (2010) Biodiversity of
658   N-cycle bacteria in nitrogen removing moving bed biofilters for freshwater recirculating
659   aquaculture systems. Aquaculture 306:177–184.

660 65. Matson EA, Brinson MM (1990) Stable carbon isotopes and the C:N ratio in the estuaries
661   of the Pamlico and Neuse Rivers, North Carolina. Limnol Oceanogr 35:1290–1300.

662 66. Law CS, Rees AP, Owens NJP (1991) Temporal variability of denitrification in estuarine
663   sediments. Estuar Coast Shelf Sci 33:37–56.

664

665 **Figure legends**

666 **Fig. 1. DIN time series.** (A) L1 (filled symbols), L2 (open symbols) and (B) H1 (filled

667 symbols), H2 (open symbols). Ammonium measurements are in blue, nitrite in green, and nitrate

668 in red. Black line denotes the sum of these nitrogen nutrients. Error bars show reproducibility of

669 duplicate measurements. Figure is modified from Babbin and Ward (5).

670

671 **Fig. 2. Instantaneous rates of anammox and denitrification.** (A) L1, (B) L2, (C) H1, (D) H2.

672 Anammox rates are shown in blue and denitrification in red. Error bars represent standard error

673 on slopes through labeled N_2 measurements.

674

675 **Fig. 3. DNA gene abundances throughout the experiment.** *Anammox 16S* (black) and *nirS*

676 (grey) abundance time courses are shown for (A) L1 and (B) H1 mesocosms. Error bars show

677 standard deviations among triplicate PCR amplifications.

678

679 **Fig. 4. Relative *nirS* abundances.** Stacked bar plot of *nirS* microarray RFRs. Purple = found in

680 both L1 and H1; Red = unique to L1; Green = unique to H1; Blue = found only in H1−38;

681 orange/yellow = in all but H1−38. Numbers indicate important archetype probes.

682

683 **Fig. 5. PCA of *nirS* microarray analysis.** A PCA plot of *nirS* probe abundances (indicated by

684 superimposed numbers) for each of the 4 samples. The same color coding is used as in Fig. 4.

685

686 **Fig. 6. Heatmap similarities among probes and metadata.** The heatmap shows how certain

687 archetype probes and environmental metadata (i.e., DIN concentrations, gene abundances, and

688 measured rates) relate to each other. The sequence of red boxes along the diagonal indicates

689 groups of highly related variables.

690

691
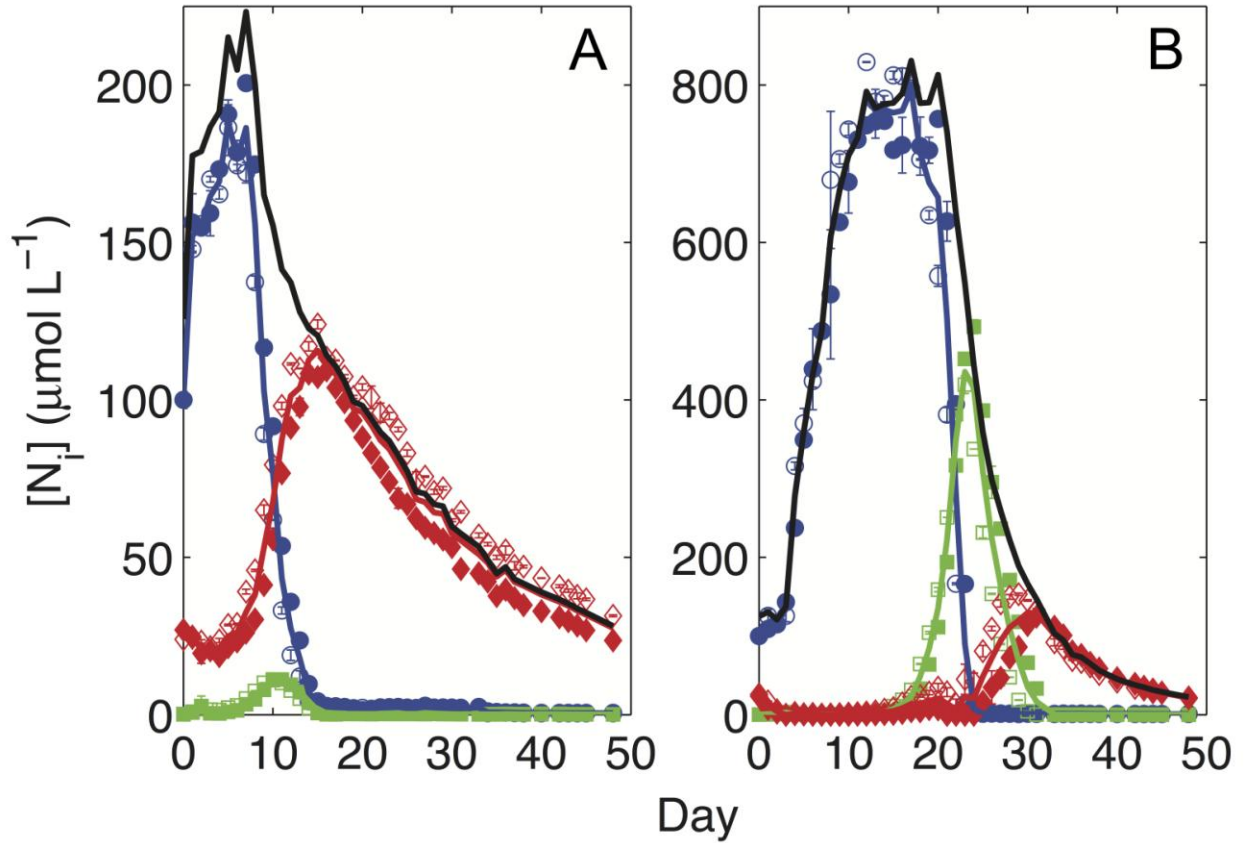
Fig. 1. DIN concentrations time series. (A) Mesocosms L1 (filled symbols), L2 (open symbols)

and (B) Mesocosms H1 (filled symbols), H2 (open symbols). Ammonium measurements are in

blue, nitrite in green, and nitrate in red. Black line denotes the sum of these nitrogen nutrients.

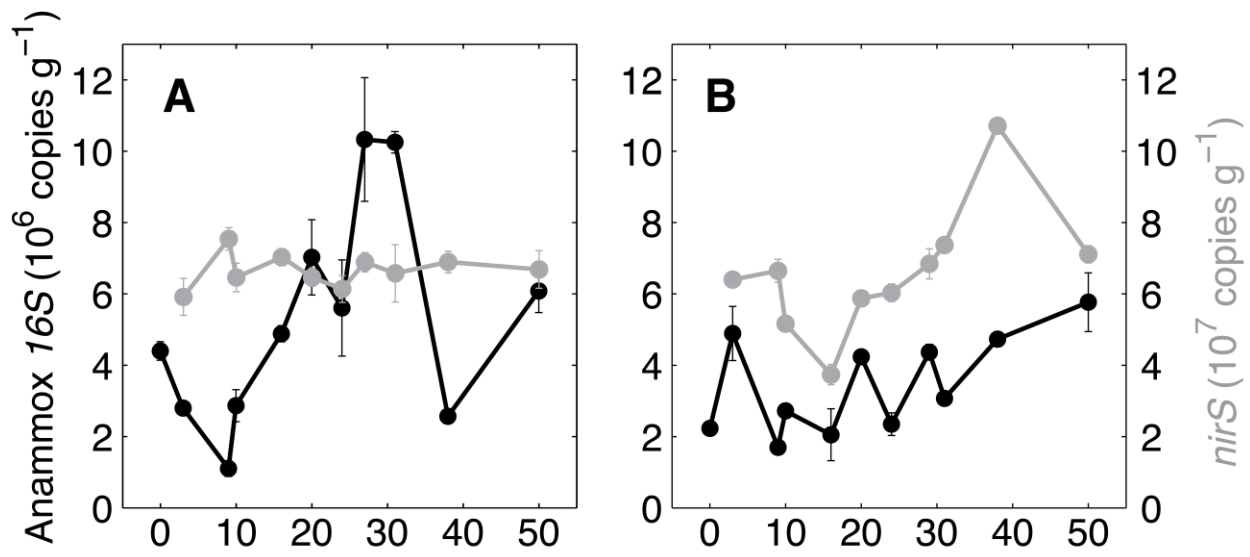Error bars show reproducibility of duplicate measurements. Figure is modified from Babbin and
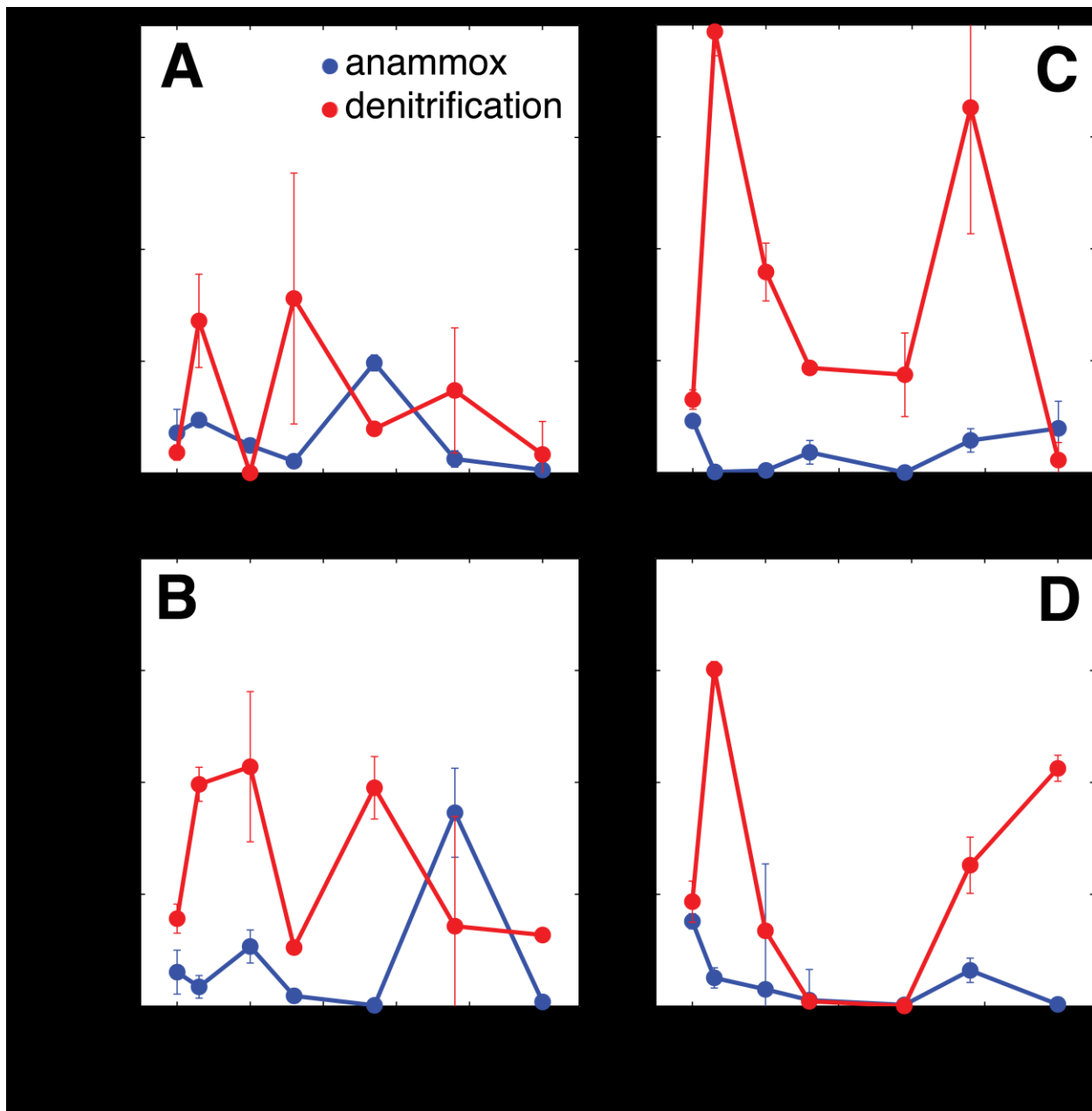
Ward (5).

697

Fig. 2. Instantaneous rates of anammox and denitrification. (A) L1, (B) L2, (C) H1, (D) H2.

Anammox rates are shown in blue and denitrification in red. Error bars represent standard error
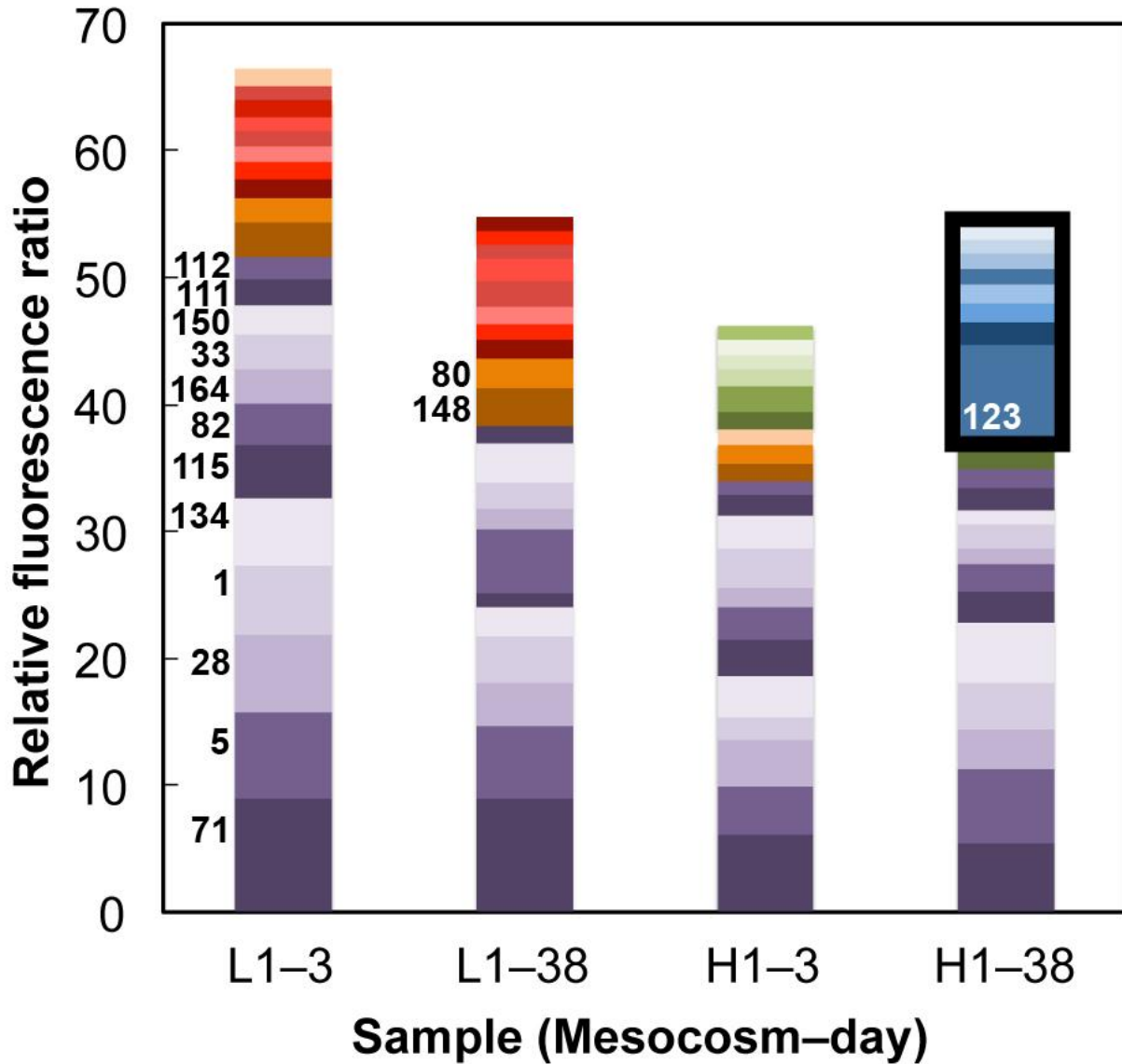
on slopes through labeled N_2 measurements.

701

Fig. 3. DNA gene abundances throughout the experiment. *Anammox 16S* (black) and *nirS*

703 (grey) abundance time courses are shown for (A) L1 and (B) H1 mesocosms. Error bars show

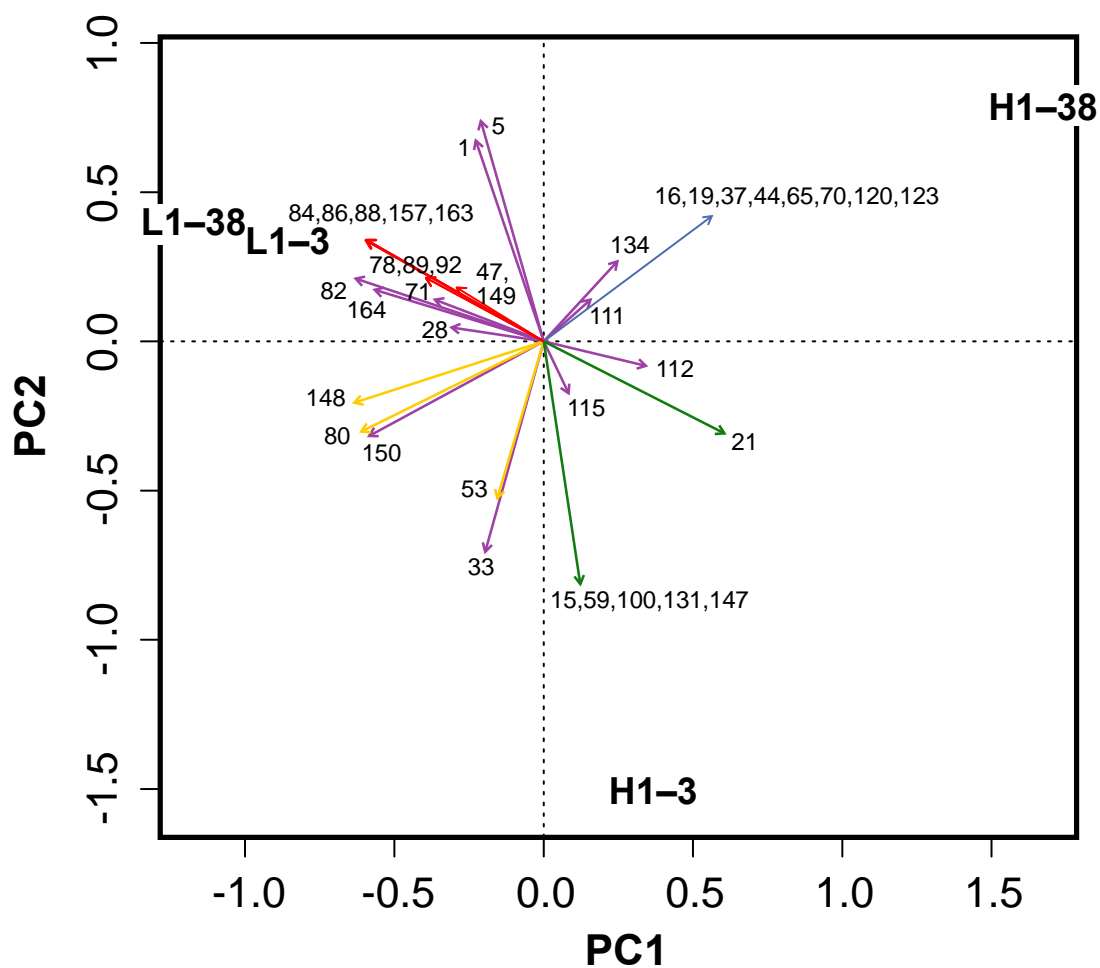704 standard deviations among triplicate PCR amplifications.

705

Fig. 4. Relative *nirS* abundances. Stacked bar plot of *nirS* microarray RFRs. Purple = found in both L1 and H1; Red = unique to L1; Green = unique to H1; Blue = found only in H1–38; orange/yellow = in all but H1–38. Numbers indicate important archetype probes.
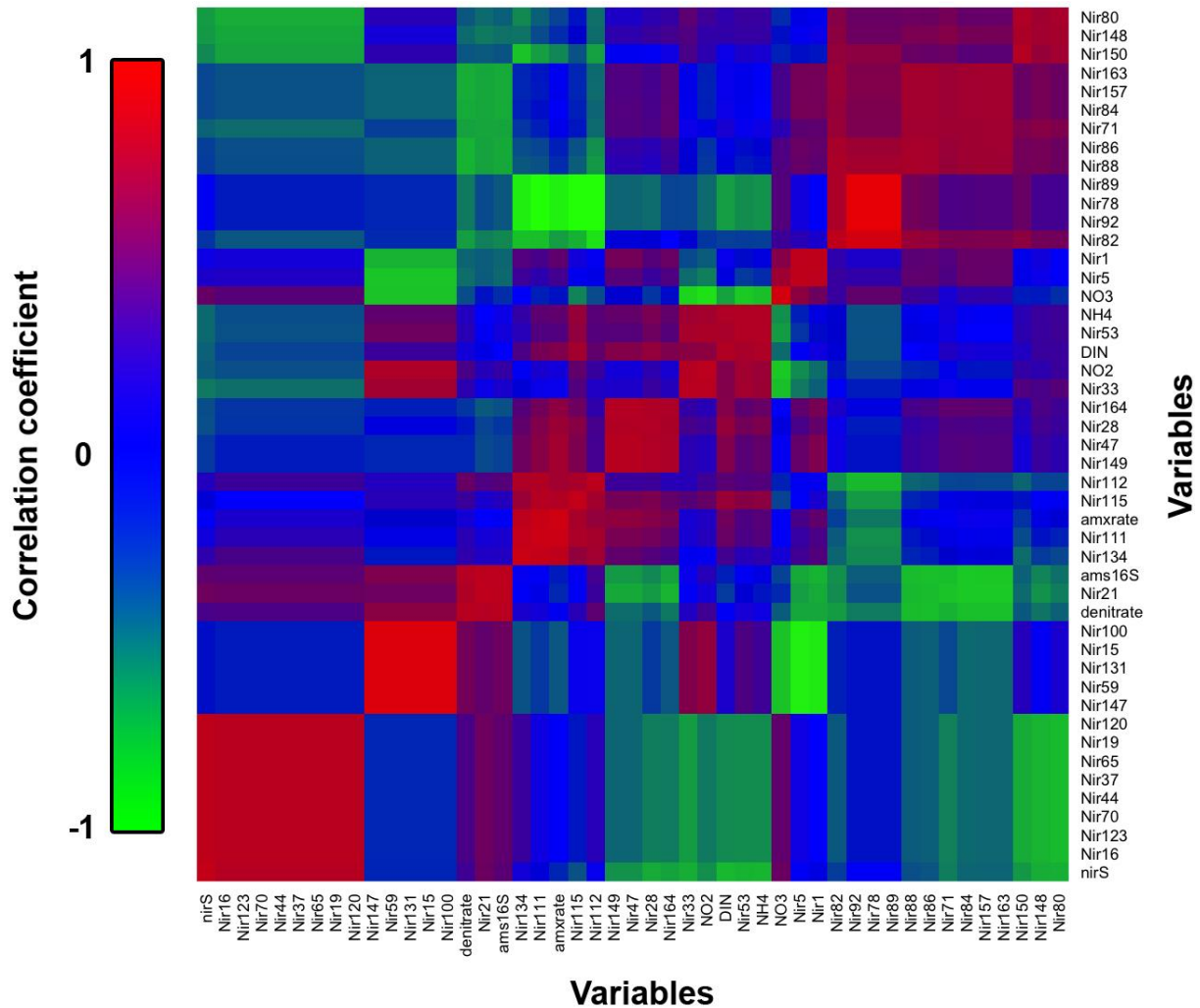
710

Fig. 5. PCA of *nirS* microarray analysis. A PCA plot of *nirS* probe abundances (indicated by

712 superimposed numbers) for each of the 4 samples. The same color coding is used as in Fig. 4.

713

714

Fig. 6. Heatmap similarities among probes and metadata. The heatmap shows how certain

archetype probes and environmental metadata (i.e., DIN concentrations, gene abundances, and

measured rates) relate to each other. The sequence of red boxes along the diagonal indicates

groups of highly related variables.